Chinese Chemical Letters 33 (2022) 4595–4599

Contents lists available at ScienceDirect

Chinese Chemical Letters

journal homepage: www.elsevier.com/locate/cclet

A GSH-depleted platinum(IV) prodrug triggers ferroptotic cell death in breast cancer

Dachuan Qi[a,1], Lei Xing[b,1], Lijun Shen[b,1], Wenshuang Sun[d,1], Cheng Cai[a], Chunhua Xue[a], Xuwei Song[a], Hua Yu[a], Hulin Jiang[b,*], Chengjun Li[d,*], Qingri Jin[c,*], Zhiqi Zhang[a,*]

[a] Department of General Surgery, Shanghai Fourth People's Hospital, School of Medicine, Tongji University, Shanghai 200434, China
[b] Department of Pharmaceutics, China Pharmaceutical University, Nanjing 210009, China
[c] Key Laboratory of Applied Technology on Green-Eco-Healthy Animal Husbandry of Zhejiang Province, College of Animal Science and Technology, College of Veterinary Medicine, Zhejiang A & F University, Lin'an 311300, China
[d] Department of Orthopedics, Jinling Hospital, School of Medicine, Nanjing University, Nanjing 210002, China

ARTICLE INFO

Article history:
Received 1 September 2021
Revised 28 March 2022
Accepted 29 March 2022
Available online 4 April 2022

Keywords:
Cisplatin
Ferroptosis
Cancer therapy
Glutathione depletion
Tetravalent platinum prodrug

ABSTRACT

Cisplatin is the first-line drug for treatment of various solid tumors including breast cancer due to the broad anti-tumor spectrum and strong anti-tumor effect. However, serious side effects and long-term medication of reduced sensitivity by high GSH in tumor cells have severely restricted its further clinical application. Herein, a GSH-depleted Pt(IV) prodrug (Platin B) based on cisplatin and 4-carboxylphenylboronic acid pinacol ester was prepared to solve the problems. As an excellent GSH scavenger, 4-carboxylphenylboronic acid pinacol ester could be activated by intracellular redox reactions to release quinone methide, thereby amplifying oxidative stress and leading to breast cancer ferroptosis therapy. Interestingly, the consumption of GSH can also reduce cisplatin inactivation, enhance the sensitivity of tumor cells to cisplatin and efficiently induce apoptosis/ferroptosis. This work highlights the use of GSH scavenger for triggering ferroptotic cell death in breast cancer.

Cisplatin is the first-line anti-cancer drug due to its broad anti-tumor spectrum and strong anti-tumor effect [1,2]. Although it has achieved great success in clinical application, its serious side effects such as nephrotoxicity and ototoxicity, as well as the reduced sensitivity caused by long-term medication, have severely restricted the clinical application of cisplatin [3,4]. To overcome various shortcomings of cisplatin, some platinum complexes were developed [5–7], however, they also have an adverse effect along with the anti-tumor effect [8]. Therefore, the development of new platinum-based drugs to improve efficacy and reduce side effect is very important and extremely desirable.

Recently, tetravalent platinum [platinum(IV)] complexes have rapidly developed as anti-tumor drugs due to their unique advantages in chemical structure, physicochemical properties and pharmacodynamic properties [9–10]. Ling *et al.* designed and synthesized a series of platinum(IV) prodrugs, and employed the reduction process of platinum(IV) for release cisplatin to consume intracellular GSH, thereby decreasing drug inactivation [11,12]. Since these modified cisplatins have demonstrated a good therapeutic efficacy, it is fascinating to further develop new modification strategies to improve the efficacy of cisplatin.

Ferroptosis is a new type of iron-dependent regulatory cell death [13], of which the mechanism is the metabolic disorder of intracellular lipid oxides based on the down-regulation of glutathione peroxidase (GPX4) [14]. Therefore, GPX4 is the key metabolic enzyme that can degrade lipid peroxides in the body, and GSH is a necessary cofactor for its enzymatic activity [15]. The regulation of GSH and GPX4 is an effective way to break the cellular redox balance, to induce the accumulation of lipid peroxides, and eventually to result in ferroptosis [16]. It was reported that ferroptosis, as a potential strategy to solve the problems of cisplatin, exhibits the excellent antitumor effect and is different from cell apoptosis pathway [17,18]. Therefore, it is a feasible and effective strategy to combine with apoptosis-induced cisplatin and ferroptosis in the treatment of tumor.

Here, we propose the development of a GSH-depleted platium(IV) prodrug with GSH depletion for efficient tumor ferroptosis therapy. This novel platium(IV) prodrug (named as Platin B) was synthesized by introducing a GSH depleting agent on

* Corresponding authors.
E-mail addresses: jianghulin3@gmail.com, jianghulin3@163.com (H. Jiang), 48933897@qq.com (C. Li), 20130017@zafu.edu.cn (Q. Jin), zzq72@163.com (Z. Zhang).
[1] These authors contributed equally to this work.

https://doi.org/10.1016/j.cclet.2022.03.105
1001-8417/

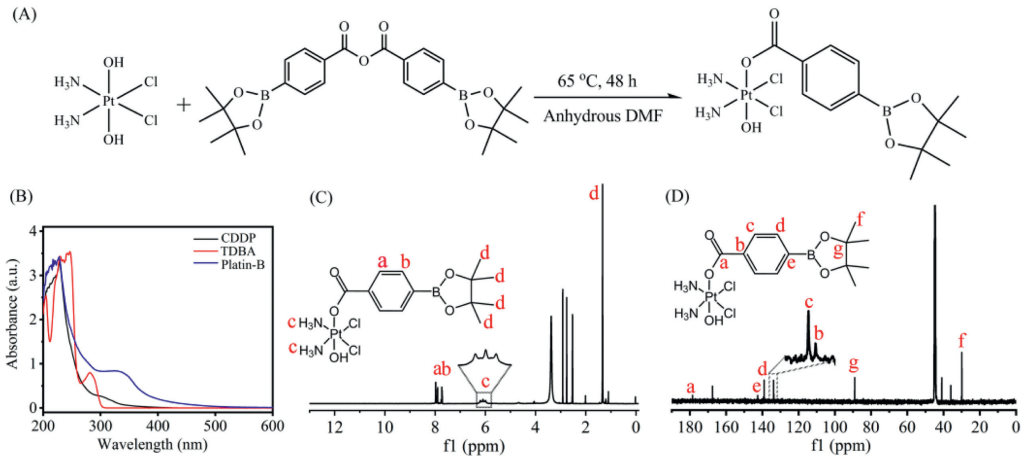

Fig. 1. (A) The synthetic route of the Platin B. (B) Ultraviolet-visible (UV-vis) spectra of CDDP, TDBA and Platin B. (C) ^{1}H NMR and (D) ^{13}C NMR of Platin B in DMSO-d_6.

the axial ligand of cisplatin. A phenylboronic acid derivative 4-carboxylphenylboronic acid pinacol ester (TDBA) [19,20] was used as the axial functional ligand to synthesize Platin B, which has dual consumption of intracellular GSH. When Platin B enters cancer cell, it is first reduced under the action of GSH to release cisplatin and phenylboronic acid derivatives. Cisplatin hydration occurs and enters the cell nucleus, inhibits DNA replication and transcription, leading to apoptosis. Cisplatin hydrate can also act on mitochondria, increasing the reactive oxygen species (ROS) and reducing mitochondrial membrane potential, which leads to cell apoptosis. Simultaneously, the released phenylboronic acid derivative interacts with H_2O_2 to generate methylquinone and further depletes the intracellular GSH. In brief, the reduction of GSH can rescue the inactivation of cisplatin, increase sensitivity of cancer cells to platinum drugs.

As shown in Fig. S1A (Supporting information), CDDP-OH was firstly synthesized through oxidizing cisplatin by H_2O_2 using the method previously reported [21]. CDDP-OH was characterized by infrared spectrum (Fig. S2 in Supporting information). Compared with the infrared characteristic peak of cisplatin (Fig. S2A in Supporting information), there was a very obvious signal peak at 3513.8 cm^{-1} (Fig. S2B in Supporting information), which was attributed to the stretching vibration of hydroxyl groups in CDDP-OH. This result demonstrated that CDDP-OH was successfully synthesized. Next, as shown in Fig. S1B (Supporting information), TDBA anhydride was firstly synthesized by dehydration condensation of TDBA using the method previously reported [22]. As shown in Fig. S3 (Supporting information), there are two C=O that can be vibrationally coupled in the structure of TDBA anhydride. The original signal peak at 1686.4 cm^{-1} in the structure of TDBA was split into two signal peaks at 1784.1 cm^{-1} and 1725.5 cm^{-1}. This is an obvious feature of the structural identification of carboxylic anhydrides, indicating that the carboxylic acid has undergone a dehydration condensation reaction to successfully generate carboxylic anhydride. The ^{13}C NMR (Fig. S4 in Supporting information) and mass spectrum (Fig. S5 in Supporting information) further confirmed the successful synthesis of TDBA anhydride.

Finally, Platin B was synthesized from esterification reaction of CDDP-OH and TDBA anhydride in anhydrous DMF at 65 °C for 2 days in the dark (Fig. 1A). Platin B was obtained as a yellow solid, which was then characterized by ultraviolet-visible (UV-vis), NMR spectroscopy and ESI-MS (Fig. S6 in Supporting information). Platin B showed different UV-vis absorption peaks from cisplatin and TDBA (Fig. 1B). The ^{1}H NMR of Platin B was shown in Fig. 1C, compared with the hydrogen spectrum of TDBA, the ^{1}H NMR of Platin B showed a triplet at 6.10 ppm, which was attributed to the NH_3 in the CDDP, and there were ^{1}H NMR peaks on benzene ring and borate ester. Furthermore, a carbon at 178.64 ppm corresponds to C=O in the Platin B structure, and the two carbons on the boron ester appear at 89.09 ppm (Fig. 1D), these characteristic absorption lines all proved the successful formation of the esterification reaction. Taken together, these results confirmed the successful synthesis of Platin B. The reason why only one hydroxyl group can react with TDBA was speculated to be the steric hindrance of TDBA and the ratio of reactants.

MTT assay was used to analyze the cytotoxicity of Platin B in 4T1 cells, and TDBA, CDDP and Mixture group (the mol ratio 1:1 mixture solution of cisplatin and TDBA) were set as controls. As shown in Fig. 2A, TDBA had no obvious inhibitory effect on the proliferation of 4T1 cells within the concentration range of 0-100 μmol/L, indicating that TDBA was not toxic within this concentration range. In addition, CDDP, Mixture and Platin B showed the obvious dose-dependent cytotoxicity. When the concentration of Platin B was 17.85 μmol/L, the cell mortality was 41%, and Platin B showed higher cytotoxicity with the increase of concentration, which was similar to the cytotoxicity of many platium (IV) drugs reduced to cisplatin (Fig. S7 in Supporting information) [22,23].

The amount of Pt in cells was determined by inductively coupled plasma-mass spectrometry (ICP-MS) to investigate the uptake of CDDP and Platin B [24–26]. As shown in Fig. 2B, both CDDP and Platin B can be successfully taken up by 4T1 cells, and the amount of drug taken up by the cells was proportional to time. In the first 2 h, the intake of Platin B was greatly increased compared with CDDP, which was 1.71 and 1.68 times higher than that of CDDP, respectively, whereas the difference in cell uptake between the two drugs gradually decreased along with cellular uptake progressing.

Next, 4T1 cells treated with Platin B were also evaluated by live/dead cell viability assays and trypan blue rejection test. As shown in Fig. 2C, the results of live/dead cell staining showed that TDBA showed complete green fluorescence after the administration and incubation, confirming that TDBA would not have a killing effect on the cells. CDDP and Mixture groups showed faint red fluorescence, demonstrating that CDDP had a certain cell killing ability. Platin B displayed a large amount of red fluorescence, manifesting that Platin B had a significant cell killing effect. The results of trypan blue staining were consistent with live/dead cell staining. There was almost no blue-violet appearance in the TDBA, while CDDP, Mixture and Platin B showed more purple, indicating a large number of cell deaths. And Platin B exhibited obvious red fluorescence, thus demonstrating that it had a significant cell killing effect, which was consistent with the result of cytotoxicity.

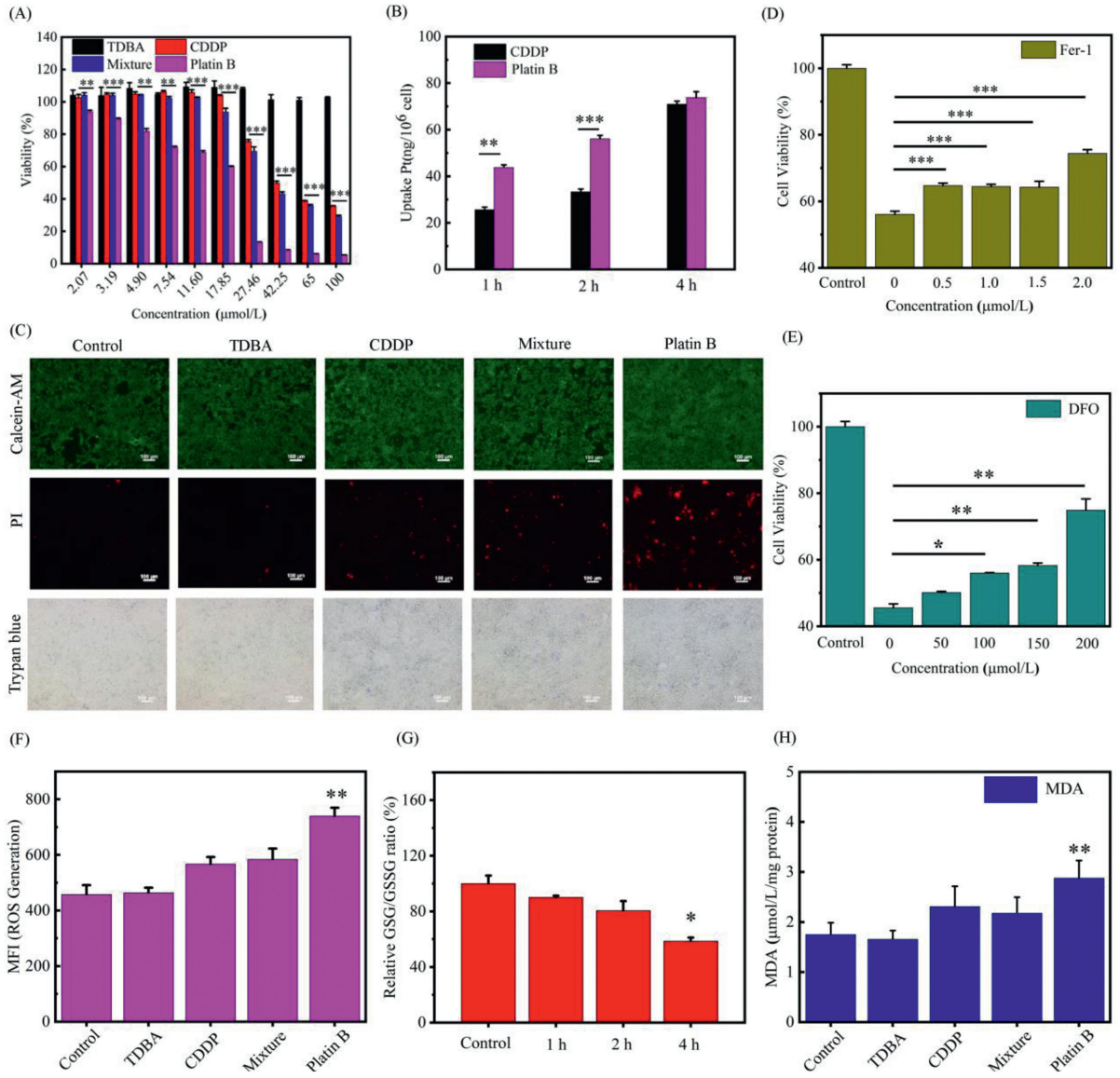

Fig. 2. (A) Cytotoxicity of TDBA, CDDP, Mixture and Platin B toward 4T1 cells. (B) Cellular uptake of CDDP and Platin B by ICP-MS. (C) Live/dead cell staining and Trypan blue staining of CDDP, TDBA, Mixture and Platin B. Viability of 4T1 cells were treated with Platin B and Fer-1 (D) and DFO (E) inhibitor. The control group was the untreated tumor cells. (F) Quantitative analysis of ROS generation by flow cytometry. (G) Value of GSH/GSSG in 4T1 cells after treatment. (H) Expression of MDA after treated with CDDP, TDBA, Mixture and Platin B.

MTT assay was also used to evaluate effects of ferroptosis inhibitor Ferrostratin-1 (Fer-1) and iron chelator deferoxamine (DFO) on cell viability [18]. As exhibited in Figs. 2D and E. Fer-1 and DFO were not added, Platin B had a strong cell killing effect. When Fer-1 was added, the cell survival rate was significantly improved, and increased significantly with the increase of the dose of Platin B. When DFO was added, the cell survival rate was also increased with increasing dose. These results indicated that Platin B can trigger ferroptosis in 4T1 cells.

Next, a flow cytometer was used to quantify the ROS generated in the cells. DCFH-DA was used as a ROS probe to investigate the production of ROS in cells [27–29]. As shown in Fig. 2F, CDDP and Mixture groups had a small amount of ROS production. After 4T1 cells were incubated with Platin B for a period of time, the green fluorescence intensity was significantly increased, suggesting that it can significantly enhance the production of intracellular ROS, and the amount of ROS production was more than that of CDDP. And there was a significant difference compared with the control. This is because Platin B consumed intracellular GSH, which was conducive to the occurrence of oxidative stress and generated a large amount of ROS to damage tumor cells.

Then, GSH and GSSG detection kits were used to determine contents of GSH and GSSG in tumor cells, respectively, to characterize the consumption of GSH by Platin B. As shown in Fig. 2G, the results demonstrated that Platin B can effectively consume intracellular GSH through the reduction process and methylquinone alkylation [19,20], and as the incubation time increased, the ratio of GSH/GSSG decreased, illustrating the more GSH in the cell was consumed by Platin B. This may be because the more it accumulated in tumor cells as the time of action of the drug increased, the more active platinum-based drug molecules played a role in the cell. Moreover, this strategy was also well documented for improving the efficacy of platinum drugs [11,12].

Malondialdehyde (MDA) is one of the important metabolites of lipid oxidation process in the cell. MDA detection kit was used to detect its content to monitor the level of lipid peroxidation caused

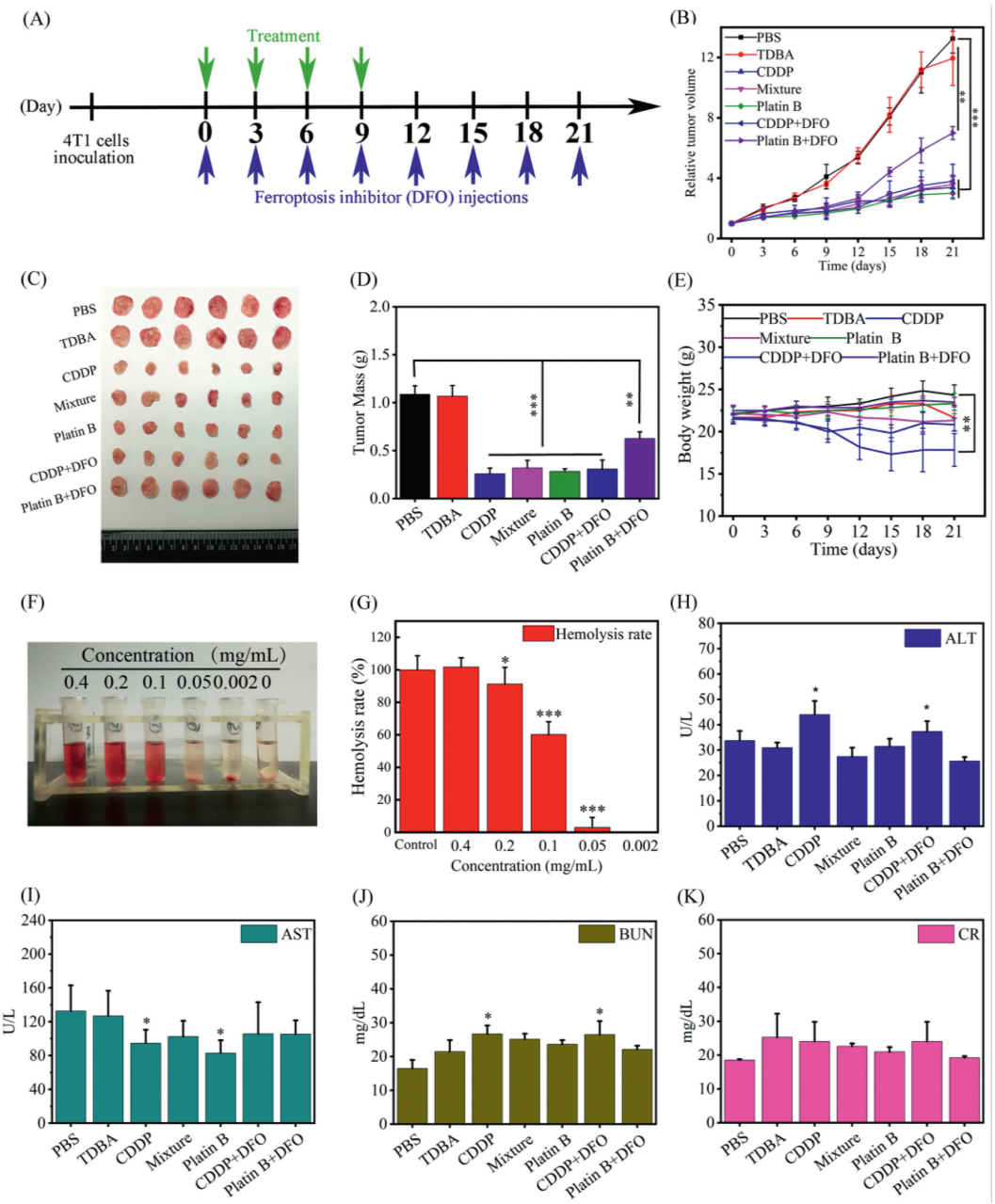

Fig. 3. (A) Therapeutic schedule of the therapeutic process. (B) Tumor growth curves after intravenous injection with various treatments ($n = 6$, $^{**}P < 0.01$, $^{***}P < 0.001$). (C) Photograph of tumor after different treatments. (D) Tumor weights after intravenous injection with various treatments ($n = 6$, $^{**}P < 0.01$, $^{***}P < 0.001$). (E) Mice body weights after different treatments ($n = 6$, $^{**}P < 0.01$). (F) Photograph of the hemolytic activity of various concentration of Platin B. (G) Relative hemolytic activity of Platin B at different concentrations ($n = 3$, $^{*}P < 0.05$, $^{***}P < 0.001$). Blood biochemistry analysis of liver function markers: alanine aminotransferase (ALT) (H), aspartate aminotransferase (AST) (I), kidney function markers: urea nitrogen (BUN) (J); creatinine (CR) (K) ($n = 6$, $^{*}P < 0.05$).

by Platin B in cells. As displayed in Fig. 2H, 4T1 cells were incubated with TDBA, there was no significant change in the content of intracellular MDA. When incubated with CDDP and Mixture groups, the content of MDA increased slightly. This was because CDDP can trigger the mitochondrial-mediated apoptosis pathway, increase intracellular ROS and oxidative stress, and raise lipid oxidation metabolites [16]. Importantly, the production of MDA after the treatment of Platin B was much higher than that of other groups. This may be due to the reduction of platin B to release CDDP, which increased intracellular ROS. Simultaneously, methyl quinone consumed GSH [19,20], which made cells more prone to oxidative damage, and lipid oxidation metabolism was more vigorous, thereby producing more MDA.

Female BALB/c mice at 6-8 weeks were used as experimental models. Animal care and handing procedures were in agreement with the guidelines evaluated and approved by the Ethics Committee of China Pharmaceutical University. The tumor volume increased to ~100 mm^3 for pharmacodynamic investigation. The tumor-bearing mice were randomly divided into 7 groups (6 in each group), which were blank control (PBS), CDDP, TDBA, Mixture, Platin B, CDDP+DFO, and Platin B+DFO group. The administration dosage was 3.5 mg/kg based on Pt, and the dose of each group remained the same. DFO was administered at a dose of 20 mg/kg by intraperitoneal injection [13]. Each mouse was given 100 μL of the drug solution by intratumoral injection, and the intraperitoneal injection of DFO solution was also 100 μL. The drug was adminis-

tered every 2 days for a total of four treatments. After the treatment, the weight change and tumor size of the mice were continuously observed and recorded. On the 21st day, the mice were subjected to orbital blood sampling, and then euthanized and major organs (heart, liver, spleen, lung, kidneys) and tumor tissues were taken out. The tumor tissue was weighed and recorded. The specific treatment plan was shown in Fig. 3A.

After inoculating tumor cells, the tumor volume of mice was observed and recorded before and after treatment. As shown in Figs. 3B and C, the tumor volume of the tumor-bearing mice was effectively suppressed after drug treatment. The change trend of TDBA and PBS group was the same, and the tumor volume increased rapidly. Both CDDP and Platin B can effectively inhibit the growth of tumors. Among them, the growth trend of Mixture and CDDP was consistent, indicating that TDBA had no effect on tumor treatment, which was consistent with the results of the cytotoxicity experiment (Figs. 2A and C). After adding DFO, there was no significant difference in growth trend compared with CDDP, indicating that CDDP had a limited ability to induce ferroptosis effect. Compared with PBS, Platin B had an obvious anti-tumor effect, and the tumor mass of Platin B+DFO was significantly increased compared with that of Platin B (Fig. 3D). This result suggested that anti-tumor effect of Platin B was weakened after adding DFO to inhibit ferroptosis. And this was consistent with the results of in vitro studies on Ferroptosis mechanisms (Fig. 2E). Taken together, Platin B had a stronger ferroptosis effect than CDDP, and led to tumor cell death through apoptosis and ferroptosis together. During the treatment, the body weight of the mice was recorded to investigate the safety of drugs (Fig. 3E). The weight change trend of Platin B and control mice was roughly the same. The slight increase in weight of PBS group may be due to the infinite increase in tumor volume, indicating that Platin B did not have an impact on the normal growth of mice. While the weight of CDDP group mice had decreased significantly, proving that CDDP had serious toxic side effect. This was also consistent with the literature reports [3,4].

The blood compatibility of the drug is an indicator that must be investigated before its application *in vivo*. As shown in Fig. 3F, after Platin B was incubated with red blood cells for a period of time, hemolysis was observed, and hemolysis was already serious when the dose was 0.1 mg/mL. The hemolysis rate of the drug was quantified by measuring the absorbance value by a microplate reader (Fig. 3G), and the result was consistent with the phenomenon observed by taking pictures (Fig. 3F). When the administration concentration was 0.1 mg/mL, the hemolysis rate was as high as 60.2%. Platin B had a certain degree of amphiphilicity, which may be the main reason for the strong hemolysis. Therefore, Platin B was used in pharmacodynamics study through intratumoral administration.

As the treatment progress, the tumor volume was effectively suppressed, indicating that Platin B had a better inhibitory effect on tumor growth (Figs. 3B and C). Meanwhile, the effects of each treatment group on the major organs should also be observed. As shown in Figs. 3H-K, the analysis of liver and kidney function indicators in the blood also showed the same experimental results, which preliminarily proved the safety of Platin B. The tumor tissue collected from the anatomy was sectioned and H&E stained to visually observe the morphological changes of the tumor tissue after the administration (Fig. S8 in Supporting information). As shown by the above results, the H&E staining of various organs also showed no significant difference between Platin B and the control, proving that it had a protective effect on important organs.

In summary, we have synthesized a new type of platinum(IV) prodrug by introducing a depleting agent of GSH in the axial position for rescuing the inactivation of cisplatin chemotherapy. After uptake of the prodrug by tumor cells, Platin B released cisplatin and phenylboronic acid derivatives under the action of GSH. Cisplatin hydration occurs and binds to DNA in the nucleus, which increased ROS and triggered apoptosis. A series of experiments *in vivo* and *in vitro* have proved that Platin B had a strong anti-tumor effect and had almost no toxic side effects. Importantly, the consumption of GSH by phenylboronic acid derivatives can also reduce the inactivation of cisplatin, enhance the sensitivity of tumor cells to cisplatin and induce ferroptosis. In brief, the platinum(IV) prodrug can overcome the tendency of cisplatin to inactivate, can be used as a new generation of platinum drug candidate and has potential application in the clinic for platinum-sensitive tumors therapy.

Declaration of competing interest

The authors declare that they have no known competing financial interests or personal relationships that could have appeared to influence the work reported in this paper.

Acknowledgments

This work was financially supported by the Priority Academic Program Development of Jiangsu Higher Education Institutions and Double First-class University Projects (No. CPU2018GY06), and Six Talent Peaks Project in Jiangsu Province (No. WSW-112) and Zhejiang province basic public welfare research project (No. LGN20C180001) and Wenzhou Engineering Research Center of Pet (No. WP02).

Supplementary materials

Supplementary material associated with this article can be found, in the online version, at doi:10.1016/j.cclet.2022.03.105.

References

[1] T.C. Johnstone, K. Suntharalingam, S.J. Lippard, Chem. Rev. 116 (2016) 3436–3486.
[2] B. Rosenberg, L. Vancamp, T. Krigas, Nature 205 (1965) 698–699.
[3] N.J. Wheate, S. Walker, G.E. Craig, et al., Dalton Trans. 39 (2010) 8113–8127.
[4] G.Y. Ho, N. Woodward, J.I. Coward, Crit. Rev. Oncol. Hematol. 102 (2016) 37–46.
[5] R.T. Penson, D.S. Dizon, S.A. Cannistra, et al., J. Clin. Oncol. 28 (2010) 154–159.
[6] J. Graham, M. Muhsin, P. Kirkpatrick, Nat. Rev. Drug Discovery 3 (2004) 11–12.
[7] J. Welink, E. Boven, J.B. Vermorken, et al., Clin. Cancer Res. 5 (1999) 2349–2358.
[8] I. Muhammad, A. Wagma, Coord. Chem. Rev. 376 (2018) 405–429.
[9] J.J. Wilson, S.J. Lippard, Chem. Rev. 45 (2014) 4470–4495.
[10] M. Patra, S.G. Awuah, S.J. Lippard, J. Am. Chem. Soc. 138 (2016) 12541–12551.
[11] L. Xiang, J.S. Tu, J.Q. Wang, et al., ACS Nano 13 (2019) 357–370.
[12] L. Xiang, C. Xing, T. Wei, et al., Nano Lett. 18 (2018) 4618–4625.
[13] S.J. Dixon, K.M. Lemberg, M.R. Lamprecht, et al., Cell 149 (2012) 1060–1072.
[14] F.R. Brigelius, M. Maiorino, Biochim. Biophys. Acta 1830 (2013) 3289–3303.
[15] W.S. Yang, R. Sriramaratnam, M.E. Welsch, et al., Cell 156 (2014) 317–331.
[16] J. Guo, B. Xu, Q. Han, et al., Cancer Res. Treat. 50 (2017) 445–460.
[17] Z. Shen, J. Song, B.C. Yung, et al., Adv. Mater. 30 (2018) e1704007.
[18] Y.J. He, X.Y. Liu, L. Xing, et al., Biomaterials 241 (2020) 119911.
[19] C.Q. Luo, Y.X. Zhou, T.J. Zhou, et al., J. Control. Release 274 (2018) 56–68.
[20] C.A. Blencowe, A.T. Russell, F. Greco, et al., Polym. Chem. 2 (2011) 773–790.
[21] E.L. Weaver, R.N. Bose, J. Inorg. Biochem. 95 (2003) 231–239.
[22] R.K. Pathak, S. Marrache, J.H. Choi, et al., Angew. Chem. Int. Ed. 53 (2014) 1963–1967.
[23] Q. Cheng, H. Shi, H. Wang, et al., Chem. Commun. 50 (2014) 7427–7430.
[24] Y. Zhu, L. Xing, X. Zheng, et al., Int. J. Pharm. 573 (2020) 118736.
[25] L. Xing, X. Chang, D. Zhao, et al., J. Control. Release 331 (2021) 460–471.
[26] C.X. Yang, L. Xing, X. Chang, et al., Mol. Pharm. 17 (2020) 1300–1309.
[27] T.J. Zhou, L. Xing, Y.T. Fan, et al., J. Control. Release 309 (2019) 82–93.
[28] T.J. Zhou, L. Xing, Y.T. Fan, et al., J. Control. Release 307 (2019) 44–54.
[29] Y.T. Fan, T.J. Zhou, P.F. Cui, et al., Adv. Funct. Mater. 29 (2019) 1806708.